

1 **Significance of sediment reverberations on receiver**
2 **functions of broadband OBS data: Comments on**
3 ***Olugboji et al.* [2016] “Nature of the Seismic**
4 **Lithosphere-Asthenosphere Boundary within Normal**
5 **Oceanic Mantle from High-Resolution Receiver**
6 **Functions”**

Hitoshi Kawakatsu,¹ and Yuki Abe^{1,2}

7 The significance of sediment layer (and also water layer) reverberations in seismic ob-
8 servation in the ocean is well recognized, and it has been one of the most challenging
9 factors that hamper investigating deeper crustal and mantle structures [e.g., *Godin and*
10 *Chapman*, 1999; *Zeldenrust and Stephen*, 2000; *Ball et al.*, 2014; *Ruan et al.*, 2014; *Bell*
11 *et al.*, 2015; *Abe and Kawakatsu*, 2015; *Audet*, 2016]. *Olugboji et al.* [2016] (hereafter

Corresponding author: H. Kawakatsu, Earthquake Research Institute, The University of Tokyo,
1-1-1 Yayoi, Bunkyo-ku, Tokyo 113-0032 JAPAN. (hitosi@eri.u-tokyo.ac.jp)

¹Earthquake Research Institute, The
University of Tokyo, Bunkyo, Tokyo, Japan.

²Hot Springs Research Institute of
Kanagawa Prefectural Government,
Odawara, Kanagawa, Japan.

12 denoted as OPKS16) has recently, however, reported in this journal about their receiver
13 function analyses of OBS data without considering this effect, and discussed about the
14 nature of the seismic LAB beneath the ocean. While such an attempt is generally a wel-
15 come one to promote OBS related research, there is some concern about how the sediment
16 reverberations might affect their results. This is a short comment on their analyses to
17 draw attention of potential OBS data users to consider and recognize the significant effect
18 of the sediment layer reverberations on OBS data.

19 The OBS data used in OPKS16 are from the Stagnant Slab Project [*Fukao et al.*, 2009]
20 in which Japanese researchers deployed broadband ocean bottom seismometers (BBOBSs)
21 in the Philippine Sea [e.g., *Isse et al.*, 2009; *Takeo et al.*, 2013]. Figure 1 shows P-wave
22 spectra of three component seismograms at a station T06, for which OPKS16 shows their
23 analysis result in their Figure 5. Spectra are calculated for 200-sec long seismograms that
24 begin at 50 sec before P-wave arrivals. Horizontal seismograms are rotated into radial
25 and transverse components, and spectra are averaged for about 50 events ($M_w > 6.0$)
26 that occurred between November, 2006 and October, 2007. The dominance of horizontal
27 components (especially the radial component) can be seen. It should be also noted that
28 horizontal component spectra show distinct peaks at ~ 0.2 Hz, ~ 0.4 - 0.5 Hz, ~ 0.8 Hz, etc.
29 that are due to reverberations of nearly-vertically traveling S-waves in the sediment layer.
30 It is possible to constrain the structure of the sediment layer by using this information
31 [e.g., *Godin and Chapman*, 1999; *Zeldenrust and Stephen*, 2000; *Abe and Kawakatsu*,
32 2015], but here we just use the frequency 0.2Hz of the fundamental resonance to obtain
33 a rough estimate of the S-wave speed of 240 m/s for an assumed thickness 300 m of the
34 sediment layer (there is a trade-off between these two parameters).

35 Synthetic receiver functions (RFs) are calculated for such a sediment layer structure,
36 and shown in Figure 2 (detailed characteristics of the effect of sediment reverberations to
37 the RF analysis will be presented elsewhere [e.g., *Abe and Kawakatsu, 2015; Audet, 2016*].
38 Synthetic seismograms (with a slowness of 0.058 s/km) are calculated for a structure with
39 a water layer ($\sim 4600\text{m}$ thick for T06) plus the sediment layer ($V_p=1600\text{m/s}$, $V_s=240\text{m/s}$)
40 over a half space ($V_p=8180\text{m/s}$, $V_s=4720\text{m/s}$) and for a structure with an additional crust
41 layer ($V_p=6780\text{m/s}$, $V_s=3660\text{m/s}$, 6km thick) just above the half space. The extremely
42 low V_s (i.e., high poisson ratio) is a general feature of marine sediment [e.g., *Hamilton,*
43 *1971; Shinohara et al., 2008*]. In addition, to compare with a potential LAB signal, a
44 discontinuity structure with a velocity reduction (10% in V_s) at a depth of 50km from
45 the sea floor is modeled. The receiver is located on the top of the sediment layer to
46 mimic the OBS observation situation. Although individual synthetic seismograms are
47 not presented here, reverberations in the sediment and water layers dominate radial and
48 vertical component seismograms, respectively, even for the case with a crustal layer. This
49 indicates that RFs obtained from radial and vertical component seismograms are also
50 dominated by the effect of reverberations. RFs are estimated by the spectral division
51 (radial over vertical) with a water level of 0.01 (a low-pass Gaussian filter with a parameter
52 $\alpha = 3$ is applied to mimic OPKS16's analyses).

53 Obtained RFs show a consistent pattern that has a positive peak at about 1 sec followed
54 by a negative peak at about 3 sec later. The initial positive peak is due to the P-to-S
55 converted phase at the bottom of the sediment layer. Because of the extremely slow S-
56 wave speed in the sediment, this wave travels almost vertically to cause a large motion in
57 the horizontal component to dominate it (as also seen in Figure 1). The direct P-wave is

58 quite weak in the horizontal component for a similar reason. As a result, the initial part
59 of the radial component is dominated by the P-to-S converted wave and its reverberation
60 phases. The second negative phase in RFs observed at about 3-sec after the initial positive
61 one is due to the first reverberation within the sediment layer, which will be followed by
62 later reverberations in a similar fashion for some time to mask many possible crustal and
63 mantle signatures; thus it is essential to model the effect of the sediment reverberation,
64 as well as that of the water layer to discuss structure further below. Note that the “LAB
65 signal” is hidden in the bottom figures in each panel of Figure 2 at about 6 sec (and later).

66 The aforementioned characteristics of the sediment layer reverberation in RF waveforms
67 can be observed in OPKS16’s analyses in their Figure S2 where they show radial RFs
68 (labeled as “without LQT rotation” on the right panel B). Here we reproduce the figure
69 as Figure 3.¹ In bottom right of Figure 3 squared by pink color, the largest positive peak
70 just before 2-sec and the largest negative phase 3-sec later resemble the pattern that the
71 sediment RFs predict (Figure 2). This indicates that the sediment reverberations are
72 likely affecting the observed RFs in OPKS16. In the left panel of Figure 3 with the LQT
73 rotation, RFs somehow become much cleaner, and positive peaks are all located at around
74 zero time. Considering that the LQT rotation is nothing but a coordinate rotation from
75 Z(vertical)/R(radial) to L(P-polarization)/Q(SV-polarization), it is not obvious how the
76 LQT rotation makes such a drastic change in RFs. For example, why the amplitude of
77 Q-RF (left panel of A) at zero time is not close to zero as expected for the Q-component
78 which is perpendicular to the incident P-wave particle motion direction (i.e., L)? Also the
79 transverse component energies (right panel of A and B), which might represent signals
80 due to structural anisotropy, are almost completely removed after the LQT rotation,

81 which seems rather unusual as the difference of the transverse component in two panels is
82 whether deconvolution is done by L (in A) or Z (in B). Furthermore, the Q components
83 show acausal energies, symmetric around the zero lag time, almost like an autocorrelation.
84 Some explanation seems necessary.² The resulting stacked RF for the station T06 in
85 bottom left of Figure 3, anyhow, shows a notable resemblance to those predicted by the
86 sediment reverberation seen in Figure 2 except for a time shift. Some clarification by
87 the authors seems to be needed. We suspect that this may not be just a coincidence and
88 that the resultant RF may somehow reflect the effect of the sediment layer reverberations,
89 which should not be interpreted as a signature from a deeper structure.

90 **Comment on the rotation from vertical-radial coordinate to LQ coordinate**
91 **for OBS data**

92 We consider this should be avoided for P-RF analyses using OBS data [e.g., *Kumar et al.*,
93 2011; *Audet*, 2016]. This is because horizontal component and the vertical component
94 records are severely affected by the signal (incoming P-wave) generated sediment-layer
95 and water-layer reverberations, respectively. As far as we deal with them separately,
96 there is a possibility of modeling their effects; but once we mix them together via LQ-
97 rotation, it seems almost impossible to model them, and the deconvolution inherent of
98 the RF analysis make it worse. Without modeling them, it seems impossible to discuss
99 the detail of the deeper structure.

Comments on OPKS16

100 We hope that the significance of sediment layer reverberations for the RF analysis of
101 OBS data has become clear, and their presence in the OBS data analyzed by OPKS16 is

102 recognized. As to comments on *Olugboji et al.* [2016], we suggest that the following points
103 should be considered seriously and further addressed by the authors.

104 1. The effect of sediment layer reverberations should be estimated and modeled first in
105 the original horizontal component seismograms for each station.

106 2. The effect of sediment layer reverberations should be then incorporated in both RF
107 analyses and waveform modeling. The effect not only affects the initial part of RFs but
108 also the later part, as the reverberations are sustained, which makes modeling for deeper
109 structure very challenging.

110 3. Although it is better to use the vertical-radial coordinate, if the authors prefer the
111 LQT coordinate, figures like OPKS16's Figure S2 (Figure 3 here) should be shown for
112 all the analyzed stations so that readers can judge the quality of RFs and the effect
113 of sediment reverberations on RF waveforms. In this case, it seems that the authors
114 need to explain how the LQT rotation cleans up RFs that allows them to make further
115 interpretation. Also all the LQ-rotated RFs should be labeled so, instead of being labeled
116 "radial" as seems to be now. Further how the rotation itself is conducted (e.g., how the
117 angles between the vertical and L/Q directions are determined) should be described.

118 4. Until all above are incorporated in the analyses, further discussions on the deeper
119 structure seem rather premature.

120 **Acknowledgments.** The first author (HK) had provided the data used in OPKS16 and
121 had an opportunity of reading early versions of OPKS16 some time between around Octo-
122 ber, 2014 and March, 2015; he had made comments to the authors about the significance
123 of the sediment layer reverberations. Unfortunately, these comments were not taken into
124 consideration by the authors, and HK feels obliged to make this comment in public. The

125 significant effect of sediment reverberations on OBS RFs deserves proper and careful treat-
126 ment, and we hope that this comment serves as a reminder in future analyses. We thank an
127 anonymous reviewer for constructive comments on the manuscript. The BBOBS records
128 of the Stagnant Slab Project are distributed by Pacific21 (<http://p21.jamstec.go.jp/>).
129 Any additional data may be obtained from the corresponding author (H. Kawakatsu,
130 hitosi@eri.u-tokyo.ac.jp).

Notes

1. It should be also noticed that the almost all RFs shown in OPKS16 are likely to be those with the LQT rotation, even though they are labeled as “radial” (e.g., Figures 5, 7, 9, 11, and many in the Supporting Information file); the vertical-radial to LQ coordinate rotation is better to be avoided in the RF analysis of OBS records as will be discussed later separately.
131
2. It is also not clear how the rotation itself is conducted (what is the reference model for it? etc.)

References

- 132 Abe, Y., and H. Kawakatsu (2015), Effects of sediment layer and shallow portion of
133 the oceanic crust on waveforms of broadband ocean bottom seismometers in northwest
134 Pacific ocean, *Abstract S23D-27777 presented at 2015 Fall Meeting, AGU, San Francisco,*
135 *Calif., 14-18 Dec.*
- 136 Audet, P. (2016), Receiver functions using OBS data: promises and limitations from
137 numerical modelling and examples from the Cascadia Initiative, *Geophys. J. Int.*, *205*,
138 1740–1755, doi:10.1093/gji/ggw111.
- 139 Ball, J. S., A. F. Sheehan, J. C. Stachnik, F.-C. Lin, and J. A. Collins (2014), A joint
140 Monte Carlo analysis of seafloor compliance, Rayleigh wave dispersion and receiver func-
141 tions at ocean bottom seismic stations offshore New Zealand, *Geochemistry Geophysics*

- 142 *Geosystems*, 15, 5051–5068, doi:10.1002/ 2014GC005412.
- 143 Bell, S. W., Y. Ruan, and D. W. Forsyth (2015), Shear Velocity Structure of Abyssal Plain
144 Sediments in Cascadia, *Seismol. Res. Lett.*, 86, 1247–1252, doi:10.1785/0220150101.
- 145 Fukao, Y., M. Obayashi, T. Nakakuki, and Deep slab project group (2009), Stagnant slab:
146 A review, *Annual Review of Earth and Planetary Sciences*, 37, 19–46.
- 147 Godin, O. A., and D. M. F. Chapman (1999), Shear-speed gradients and ocean seismo-
148 acoustic noise resonances, *J. Acoust. Soc. Am.*, 106, 2367–2382.
- 149 Hamilton, E. L. (1971), V_p/V_s and Poisson’s ratios in marine sediments and rocks, *J.*
150 *Acoust. Soc. Am.*, 66, 1093–1101, doi:10.1785/0220150101.
- 151 Isse, T., H. Shiobara, Y. Tamura, D. Suetsugu, K. Yoshizawa, H. Sugioka, A. Ito, M. Shino-
152 hara., K. Mochizuki, E. Araki, K. Nakahigashi, H. Kawakatsu, A. Shito, T. Kanazawa,
153 Y. Fukao, O. Ishizuka, and J. B. Gill (2009), Seismic structure of the upper mantle
154 beneath the Philippine Sea from seafloor and land observation: implications for man-
155 tle convection and magma genesis in the Izu-Bonin-Mariana subduction zone, *Earth*
156 *Planet. Sci. Lett.*, 278, 107–119.
- 157 Kumar, P., H. Kawakatsu, M. Shinohara, T. Kanazawa, E. Araki, and K. Suyehiro (2011),
158 P and S receiver function analysis of seafloor borehole broadband seismic data, *J. Geo-*
159 *phys. Res.*, 116, B12,308, doi:10.1029/2011JB008506.
- 160 Olugboji, T. M., J. Park, S. Karato, and M. Shinohara (2016), Nature of the Seismic
161 Lithosphere-Asthenosphere Boundary within Normal Oceanic Mantle from High- Res-
162 olution Receiver Functions, *G-cubed*, *in press*, doi:10.1002/2015GC006214.
- 163 Ruan, Y., D. W. Forsyth, and S. W. Bel (2014), Marine sediment shear velocity structure
164 from the ratio of displacement to pressure of Rayleigh waves at seafloor, *J. Geophys.*

165 *Res.*, 119, 1–14, doi:10.1002/2014JB011162.

166 Shinohara, M., T. Fukano, T. Kanazawa, E. Araki, K. Suyehiro, M. Mochizuki, K. Nakahi-
167 gashi, T. Yamada, and K. Mochizuki (2008), Upper mantle and crustal seismic structure
168 beneath the northwestern Pacific basin using a seafloor borehole broadband seismometer
169 and ocean bottom seismometers, *Phys. Earth Planet. Inter.*, 170, 95–106.

170 Takeo, A., K. Nishida, T. Isse, H. Kawakatsu, H. Shiobara, H. Sugioka, and T. Kanazawa
171 (2013), Radially anisotropic structure beneath the Shikoku Basin from broadband sur-
172 face wave analysis of ocean bottom seismometer records, *J. Geophys. Res.*, 118, 1–15,
173 doi:10.1002/jgrb.50219.

174 Zeldenrust, I., and R. A. Stephen (2000), Shear Wave Resonances in Sediments on the
175 Deep Sea Floor, *EOS, Trans., AGU*, 81(48), *Fall Meet. Suppl.*, Abstract S51B-04.

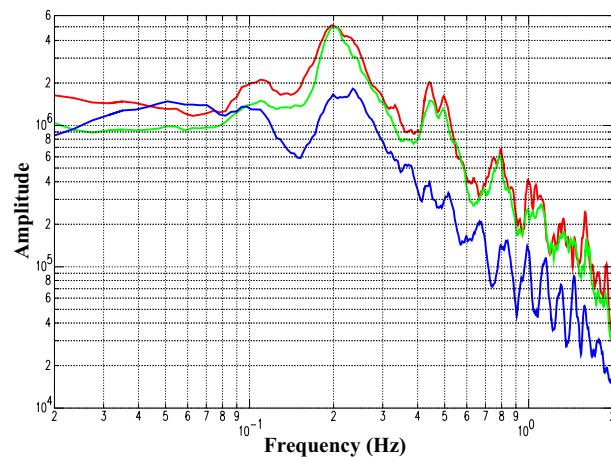


Figure 1. P-wave velocity spectra at station T06. Vertical (blue), radial (red) and transverse (green) component spectra are shown.

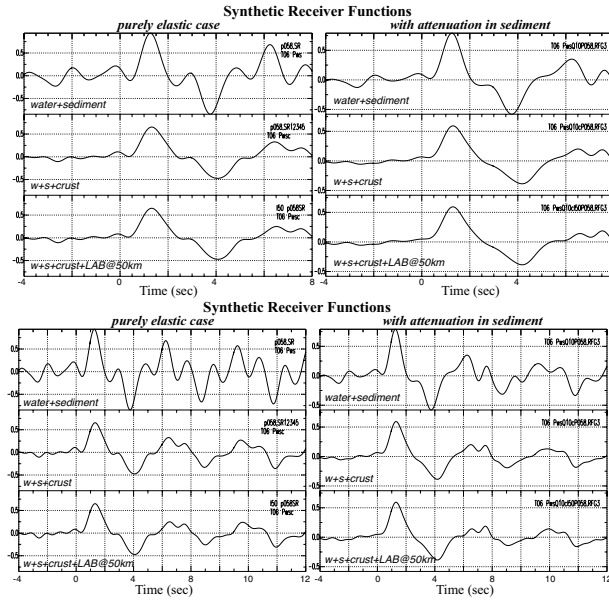


Figure 2. Two panels show the same synthetic radial RFs for station T06 with water and sediment layers over a half space (top), with an additional crust just above the half space (middle), and with an additional LAB structure (a velocity reduction of 10% at 50km from the sea floor) (bottom). RFs of a purely elastic case are shown on left, and those with inelastic sediment layer ($Q_s = 10$) are shown on right. The upper panel shows for a time window comparable to that of Figure 3, and the lower one for a longer time window to appreciate the reverberation effect. Note the consistent pattern of a positive phase at around 1-sec, followed by a negative phase 3-sec later. The exact timing of phases depends on the detail of the sediment structure, but the pattern is expected whenever there is a substantial sediment layer.

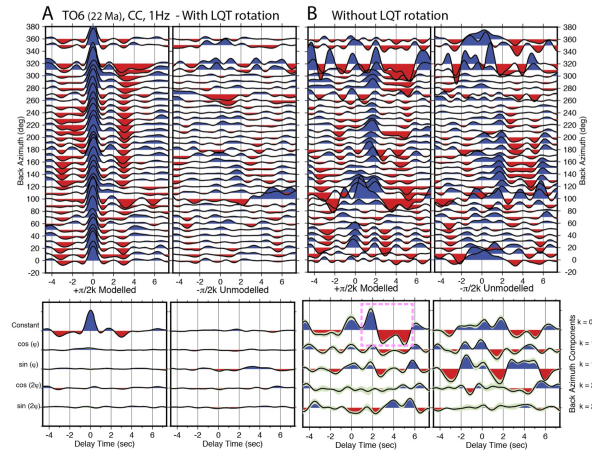


Figure 3. RFs of OPKS16 for station T06 (reproduction of their Figure S2). A box with broken pink lines indicates radial RFs that show the pattern predicted by the sediment reverberations.